BOSQUE 45(2): 359-371, 2024 DOI: 10.4067/S0717-92002024000200359

Remote sensing of forest fine-scale gap dynamics: A case study on lenga beech forests in Argentina

Teledetección a escala fina de la dinámica de claros: el boque de *Nothofagus pumilio* en Argentina como caso de estudio

Violeta Kotova [a,b], Gastón Díaz [c,d*], Diego Mohr Bell [c], Stefan Zerbe [a,e]

[a] Free University of Bozen-Bolzano, Faculty of Agricultural, Environmental and Food Sciences, Bozen, Italy.

[b] University of Innsbruck, Institute of Geography, Innsbruck, Austria.

* Corresponding author: [c] Centro de Investigación y Extensión Forestal Andino Patagónico (CIEFAP), Esquel, Argentina, gdiaz@ciefap.org.ar

[d] Consejo Nacional de Investigaciones Científicas y Técnicas (CONICET), Buenos Aires, Argentina.

[e] Institute of Geography, University of Hildesheim, Hildesheim, Germany.

ABSTRACT

The Andean Patagonian forests are characterized, on the one hand, by a high degree of naturalness and, on the other hand, by signs of degradation by grazing, unsustainable timber use, the invasion of non-native tree species and anthropogenic fire. Considering the large extent of these forests and the variety of uses, traditional forestry practices should be revised in light of modern technologies. We employed Landsat time series from 1998 to 2020, accompanied by Landsat images from 1985, 1986, 1987, and 1992 to detect the fine-scale gap dynamics of *Nothofagus pumilio* forests in central Patagonia, Argentina. These gaps can occur naturally (*i.e.* death of old trees) or can be anthropogenically induced (*i.e.* after logging). In total, 41 permanently established study plots covering an area of 40 ha were investigated. Our aim was to test the viability of the TimeSync method for detecting fine-scale disturbances. This method was proposed in 2010, and up to date, it has only been employed to study vegetation disturbance of a scale that affects several pixels. Our adaptation of the TimeSync method proved to be useful in identifying the time and intensity of changes in tree structure at the pixel scale. Accordingly, it can support forest monitoring and management by providing a cost-effective proxy for natural dynamics.

Keywords: best Available Pixel, deadwood, forest inventory, Landsat images, TimeSync method.

RESUMEN

Los bosques andino-patagónicos están caracterizados por haber sido poco intervenidos por el hombre, pero también por mostrar signos de degradación por pastoreo, explotación maderera, invasión de especies exóticas y fuegos de origen antrópico. Considerando la gran extensión de estos bosques y la variedad de usos, las prácticas forestales tradicionales deberían revisarse a la luz de las tecnologías modernas. Con las restricciones dadas por la disponibilidad de imágenes de archivo, analizamos series temporales Landsat comprendidas entre 1998 y 2020, acompañadas por imágenes Landsat de 1985, 1986, 1987 y 1992, con el objetivo de detectar la dinámica de claros que ocurre a escala fina en el bosque de *Nothofagus pumilio* de la región andino-patagónica central de Argentina. Estos claros pueden ocurrir naturalmente (*i.e.* muerte de árboles viejos) o pueden ser antropogénicos (*i.e.* raleos). En total, se investigaron 41 puntos establecidos permanentemente en un predio de 40 ha. Nuestro objetivo fue evaluar la viabilidad del método *TimeSync* para detectar disturbios de escala fina. Este método fue propuesto en 2010 y, a la fecha, fue solamente empleado para estudiar disturbios en la vegetación de una escala tal que afectan varios píxeles. Nuestra adaptación del método *TimeSync* demostró utilidad para identificar el tiempo e intensidad de los cambios en la estructura forestal a escala de píxel. Debido a ello, el método podría contribuir al monitoreo y manejo del bosque al proveer una variable proxy, muy económica de medir, de las dinámicas naturales.

Palabras clave: mejor píxel disponible, madera muerta, inventario forestal, imágenes Landsat, método TimeSync.

INTRODUCTION

Forests are globally under the focus of environmental policy regarding climate change mitigation, carbon sequestration, and biodiversity conservation, and also provide many other ecosystem services (Brockerhoff *et al.* 2017). Accordingly, forest restoration and sustainable forest management are part of the global environmental agenda. In addition to socioeconomic preconditions, ecological site conditions and natural or anthropogenic forest dynamics are important basis for sustainable forest management. Consequently, forest inventories have been developed worldwide, following a defined protocol and increasingly applying remote sensing (Seppi *et al.* 2022).

Temperate forests in all regions of the globe have been strongly transformed by anthropogenic activities (Pugh *et al.* 2024). In addition to land use change and deforestation, existing forests have been degraded to a large extent (Ghazoul and Chazdon 2017). Forest degradation encompasses a decline in biodiversity and carbon sequestration in the above- and below-ground ecosystem compartments and a change from natural to anthropogenic dynamics, with trade-offs for the socio-economy from the regional to the national level.

Argentinian Andean Patagonian forests, which extend approximately 2,000 km north of the Neuquén Province to Isla de los Estados, are one of the last global reserves of temperate forests with relatively low anthropogenic alterations and high biodiversity (Pacha *et al.* 2007). However, these forests are increasingly degraded by grazing (Zeberio and Pérez 2020), unsustainable timber use (Zerbe *et al.* 2023), invasion of non-native tree species such as *Pseudotsuga menziesii* (Mirbel) Franco (Salgado Salomón *et al.* 2013) and anthropogenic fires (Mundo *et al.* 2017). This trend is leading to an undesirable loss of ecosystem services.

Forest disturbances and dynamics vary in terms of triggering factors, extent, and frequency. Triggering factors include natural and anthropogenic factors, such as *i.e.* storms, fire, drought, timber logging, forest grazing, and infrastructure construction (Sturtevant and Fortin 2021). Accordingly, qualitative and quantitative analysis of forest dynamics has become a key aspect of the monitoring of forests and sustainable forest management (Hirschmugl *et al.* 2017). Disturbance-based management that mimics natural ecological processes is considered to sustain ecosystem functions and dynamics, while maintaining biodiversity and ecological resilience (Amoroso and Blazina 2020). Natural dynamics that are particularly challenging to mimic during management include those with frequent small-scale disturbances. Fine-scale gap dynamics mostly affect individual trees (McCarthy 2001).

Reliable and cost-efficient methods are essential to assess forest dynamics. The lack of up-to-date and comprehensive national forest inventories in many countries, for example, has raised concerns regarding the accuracy of the resulting statistics on forest area change at the global level (Ramírez *et al.* 2022). A more advanced use of satellite images has been suggested to fill this gap (Baker *et al.* 2010). Remote sensing technologies have improved our long-term understanding of forest dynamics, and have been increasingly applied since the 1970s. Passive optical multispectral satellite sensors provide consistent and reproducible measurements at a spatial scale that is appropriate for capturing the effects of many processes that cause change, including natural and anthropogenic disturbances (Kennedy *et al.* 2007).

The Landsat satellite imagery archive is suitable for the analysis of forest dynamics at medium spatial and temporal resolutions, offering a unique long-time series starting from the 1970s (Townshend and Justice 1988), particularly since the Landsat archive has become freely accessible (Wulder *et al.* 2012). The Landsat archive provides robust standardized image products that have been radiometrically and geometrically pre-processed, thus enabling the generation of cloud-free radiometric consistent composites (White *et al.* 2014). This has also catalyzed the development of time-series analysis approaches (for example, Huang *et al.* 2010, Kennedy *et al.* 2010). These approaches make better use of the temporal depth of the Landsat archive, intending to reconstruct forest disturbance histories and forest dynamics, as well as forest regeneration and succession (Novo-Fernández *et al.* 2018).

The Landsat-based detection of trends in disturbance and recovery (LandTrendr) algorithm was among the first approaches to take advantage of annual time series (Kennedy *et al.* 2010). LandTrendr uses temporal segmentation to capture a wide range of forest change processes, ranging from abrupt disturbances and chronic mortality to varying rates of vegetation recovery. Similar to most methods, the development of LandTrendr required reference data. In this case, it required high-quality vegetation dynamics data along the chosen time window (decades), but the availability of these data was and still is very rare. To address this, Cohen *et al.* (2010) developed TimeSync to facilitate accurate assessment of Landsat time-series analysis. TimeSync was presented as a tool for the visual interpretation of time series. Accordingly, TimeSync is a complementary method to LandTrendr and can be applied to validate the time series generated automatically by the latter (Kennedy *et al.* 2007, 2010).

Using TimeSync, a trained interpreter can manually define different change classes by interpreting pixel data within spatial, spectral, and temporal contexts (Banskota *et al.* 2014). Studies have proven that this approach is a valuable tool for analyzing and reconstructing disturbance regimes and forest dynamics (Cohen *et al.* 2010). However, it is not clear whether this approach can be used to characterize fine-scale gap dynamics (fine-scale refers to disturbances that do not remove the entire forest overstory at the pixel scale). Therefore, as a proof of concept, we tested the TimeSync method for the detection of fine-scale gap dynamics in the mountain forests of Patagonia (testing an automatic algorithm is out of the scope of this study). Here, we hypothesize that the annual fine-scale gap dynamics of *Nothofagus* forests in northern Patagonia can be detected using a time series of Landsat images from 1985 to 2020 and by applying an adapted TimeSync methodology. Based on this remote sensing approach and field visits, we discuss the potential for forest inventory and monitoring by integrating remote sensing and field data.

METHODS

Study area. The study area covers the Huemules Norte Experimental Unit of the National University of Patagonia San Juan Bosco (UNPSJB), located 26 km northwest of the city of Esquel in the Chubut Province of Argentina. The experimental unit is located on the mountains of Cordón Rivadavia (figure 1) and is mainly used to train forestry students in silvicultural practices. The climate of the study area is cool temperate, with a mean annual temperature of approximately 12 °C and prevailing winds from the west, bringing moisture and rain from the Pacific Ocean.

Among the 20 tree genera found in these Southern Hemisphere forests, 90 % of the total area is occupied by species of the genus *Nothofagus* (CIEFAP and MAyDS 2016). The study area is covered with pure *Nothofagus pumilio* (Poepp. & Endl.) Krasser forest stands with an extension of 40 ha. The mean forest metrics obtained from a traditional forest inventory conducted in 2013 by UNPSJB students were 13.9 m total height, 38.7 cm quadratic mean diameter and 40.3 m^2 basal area. *N. pumilio* is commonly known as a lenga or lenga beech (Armesto *et al.* 1992). Lenga beech is a broad-leaved deciduous tree species widely distributed in Argentinian Andean Patagonia, from latitude 36° to 55° S, and from sea level up to 2,000 m a.s.l., dominating high elevation stands in north and central Patagonia. Lenga forests provide multiple ecosystem services, thus gaining extraordinary importance for the country (Quinteros 2018). The common management practice of these forests has been selective logging for timber, which means the removal of the best-featured individual trees. This forestry use has been accompanied by agricultural use in the form of forest grazing, thus becoming a silvopastoral system.

Remote sensing approach and fieldwork. The locations of 41 permanently established study plots from the Huemules Norte Experimental Unit were used. Figure 2 shows the distribution of the study plots, with nine transects coded from A to I. Each study plot within each transect was numbered from 1 to 5. The centers of the study plots were established within a few meters of error (< 5 m) using differential correction GPS. These positions were used in the laboratory to extract the reflectance values from the multispectral remote sensing images, while a circular plot area (10 m radius, 314 m^2) was used in the field to interpret forest dynamics at a scale related to pixel size. To complement these upscaling efforts, we used a true-color image generated by drone-based photogrammetry (Díaz *et al.* 2020). These data, surveyed on November 21, 2016,

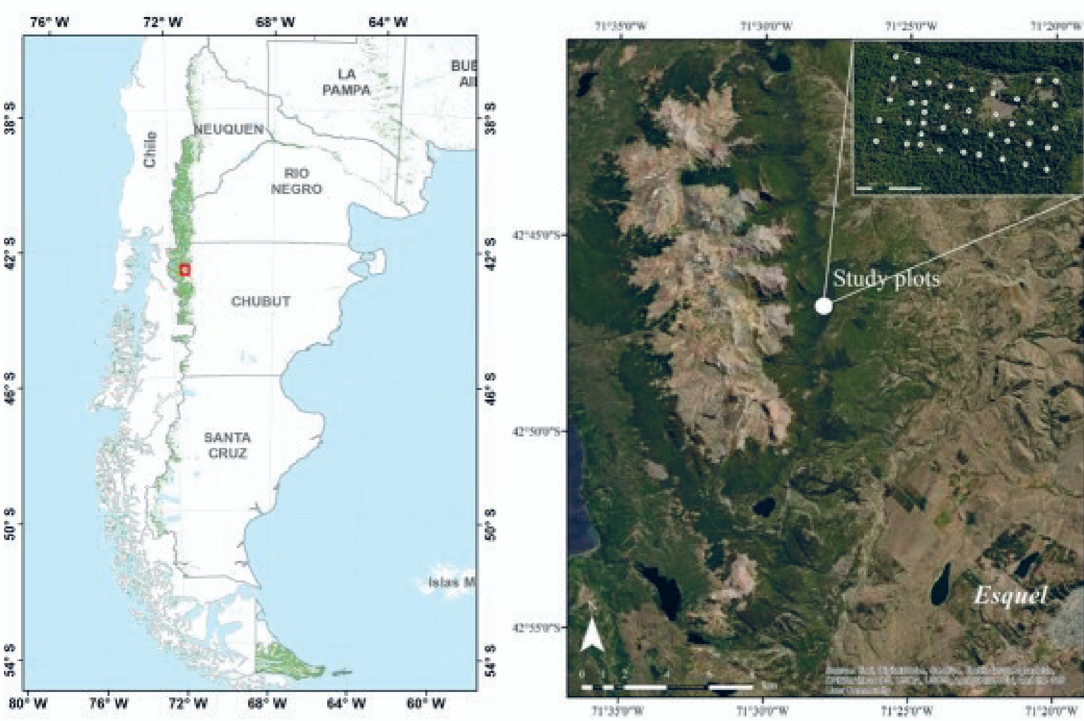

Figure 1. Study area Huemules Norte Experimental Unit on the Cordón Rivadavia mountain range, showing the location in Patagonia, with a zoom in on the experimental plots (figure 2 for a close-up). The green area represents land covered by Native Forest in Argentina according to the land cover classification by CIEFAP and MAyDS (2016).

Localización en Patagonia del área de estudio Unidad Experimental Huemules Norte del Cordón Rivadavia, y una ampliación de las parcelas experimentales (figura 2 muestra un acercamiento). Las área pintadas de verde representan suelo cubierto por bosques nativos de acuerdo con la clasificación de la cobertura del suelo realizada por CIEFAP y MAyDS (2016).

supported our research by providing a high-resolution top view of the canopy that facilitates human interpreters to link field examination with multispectral Landsat images. Hereafter, we will refer to this true-color image as the unmanned aerial vehicle (UAV) orthomosaic.

Overall, our adaptation of the TimeSync method involved three steps: (1) field examination of the study plots, (2) production of Landsat image composites, and (3) analysis of the time-series data. These steps are explained in detail in the following paragraphs.

The field examination was conducted in February 2020 and encompassed a description of the study plots and on-site detection of logging operations or natural disturbances (*i.e.* dying of trees). Tree canopy density and presence of tree regeneration were assessed visually. The development phase was assigned the label "mature" when the forest patch was beyond the self-thinning phase, or "young" otherwise. We also observed that mature forest stands have dead branches in the canopy (branch dieback), a fact that proved useful in remote sensing, as explained in the Results section (figure 3).

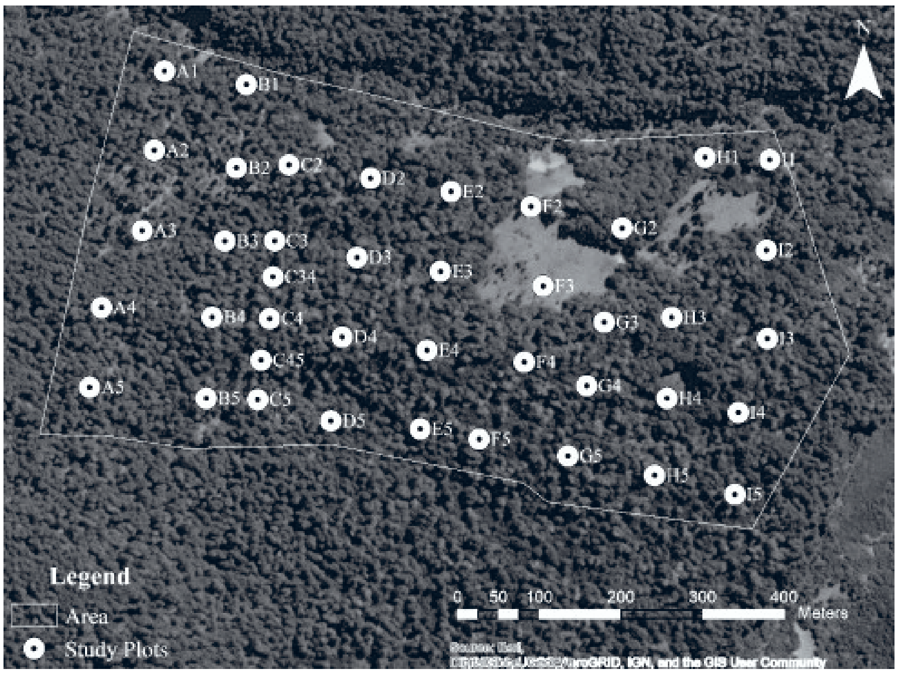

Figure 2. Labelled study plots, the centre of each is used for building the time series. Date of the ESRI base image: 26.03.2018.

Parcelas experimentales etiquetadas, su centro fue utilizado para construir las series temporales. Fecha de la imagen ESRI de base: 26.03.2018.

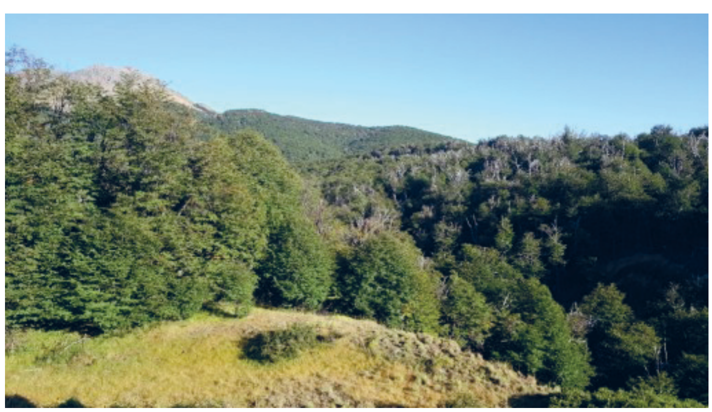

Figure 3. The photograph gives a view over the vegetation on part of the study area and northeast of it. It shows the presence of dead branches on the mature *Nothofagus pumilio* trees associated with the analysis. Date: 28.02.2020. Photo by V. Kotova.

Fotografía mostrando una vista de parte de la vegetación del área de estudio y la zona al noroeste de la misma. Muestra la presencia de madera muerta en los árboles maduros de Nothofagus pumilio asociados con el análisis. Fecha: 28.02.2020. Foto por V. Kotova.

To obtain the Landsat image composite, we applied the method of White *et al.* (2014) implemented in the *geebap* package (Principe 2017) in order to obtain one composite per year from the Landsat archive. With restrictions imposed by image availability, we worked from 1998 to 2020, 1985, 1987, and 1992. For this study, we chose to design an annual composite to include only data from a suitable phenological window, from December 1st to March 15th, which corresponds to the summer in the southern hemisphere temperate zone. We combined the time window with the target day of the year (target DOY), sensor preferences, distance to cloud, and percentage of cloud cover. These are parameters implemented in the *geebap* package and taken from White *et al.* (2014), except for the percentage of cloud cover. The percentage of cloud cover score is calculated with the cloud classification layer provided with the product (Foga *et al.* 2017) and a simple rule that we will explain with an example: if there is a cloud that occupies 20 % of the scene, every pixel classified as a cloud will have a score of 0.2, while the rest, 0.8. Finally, after adding all the scores, the algorithm looked for the best-scored pixel (presumably the best available pixel, BAP) to make the image composite.

After obtaining the composites, the normalized difference vegetation index (NDVI) was calculated as follows:

$$NDVI = \frac{NIR - Red}{NIR + Red} \quad [1]$$

were *NIR* is the near infrared band values and *Red* the red band values.

In summary, the output was an NDVI profile (the time series) and Landsat imagery stacks for visual interpretation.

According to Hirschmugl *et al.* (2017), the TimeSync method is trajectory segmentation approaches that, as such, propose to interpret vegetation dynamics with a simple model consisting of a polyline in which each vertex indicates the start and end of a period of disturbance or regrowth. This method is strongly based on visual interpretation and expert criteria.

Applying this method to detect fine-scale gap dynamics presents specific challenges. First, forest heterogeneity is large, as demonstrated by the texture diversity shown in figure 2. Consequently, remote sensing noise cannot be reduced by averaging a value from a 3 × 3 pixel size window, as the original TimeSync method have proposed. Here, we instead propose using the nearest pixel value along with a complementary method to help the interpreter handle noise in the signal by automatically detecting outliers. Essentially, this method offers a simple way to quantify the residual component, as mentioned by Hirschmugl *et al.* (2017). We explain the detection of outliers in three parts.

Firstly, the identification of the outliers was carried out by identifying the study plots that showed stability during the entire time series (hereafter, the undisturbed plot). This was performed based on field notes, expert knowledge, and time-series interpretation. To show how far each NDVI value is from its mean, but based on the standard deviation of the undisturbed plot, we proposed to calculate a z-score as follows:

$$z = \frac{NDVI - \overline{NDVI}}{\sigma} \quad [2]$$

where z is the z-score, *NDVI* is the vegetation index value of a given plot in a given year, $\overline{NDVI}$ is the mean NDVI value of the time series of that plot, and σ is the standard deviation of NDVI values from the undisturbed plot.

Second, if the z-score of an NDVI value is more than 1.5 units, it indicates that the data point is significantly different from the other data points. Such a data point was classified as an outlier, which means that it could be a meaningful vegetation change, and should be examined closely to be explained. Thus, we cleared gross technical errors in the data, such as Landsat 7 satellite failure and cloud distortion.

Third, the rest of the marked values were examined by visual analysis of the Landsat imagery, cross-referencing it with the available field data and additional knowledge about the former management of the study area obtained by unstructured interviews with CIEFAP and UNPSJB professionals. The result was trajectory segmentation manually drawn on top of each time series.

Data extraction and data analysis customized routines were written in Python 3.6 (Python Software Foundation 2021) and the open-source web application Jupyter Notebook (Project Jupyter 2021). The Google Earth Engine web interface and ArcGIS 10.7.1, were used as accompanying tools to examine the composites, modify, and present the study plots.

RESULTS

Six categories were defined after simultaneous examination of the field description and Landsat imagery obtained for each plot (table 1). During the examination, common characteristics were observed in the remote-sensing data, which were then confirmed using the field description of the plots.

The study plots with young dense forest stands were easily identified by its intense bright red palette of the traditional false-color representation (near-infrared, shortwave infrared, and red, respectively, assigned to the RGB channels). Either following a crown reduction season seen in the time series or following a reduction phase before the time series, the vegetation state is noticed as a recovery with a dense second-age class layer. This color palette is distinguishable for young forest patches, but also for increasing leaf area and photosynthesis of mature trees, which react to available resources. The absence of a second tree layer (regeneration) makes it easier to spot crown reduc-

Table 1. Forest structures found after data set examination.

Estructuras forestales que se desprenden del análisis del set de datos.

Group N°	Forest development phase	Tree canopy density	Presence of regeneration	Number of study plots in the categories[1]
1	Mature	Moderately dense	Yes	5
2	Mature	Moderately dense	No	4
3	Mature	Dense	Scarce	5
4	Mature	Dense	Yes	10
5	Mature	Dense	No	5
6	Young	Dense	No	11

[1] One of the 41 plots is an open area and has no forest coverage and thus, does not fall into the 6 categories.

tion in the mature stand, as there is no other vegetation apart from the mature trees to impact on the NDVI values.

The presence of dead branches on the mature trees makes the identification of mature stands easier because of the decrease in color saturation, as was easily confirmed by the joint analysis of the UAV orthomosaic and the Landsat stacks.

Interpretation examples. Examples were chosen because they are the most representative of their group and are a good example to show the color palette of the Landsat imagery in different groups with different dynamics. Each example presents an NDVI profile with values for each year smoothed with a moving average of 2 years. In addition to these values, green line segments were drawn over the points to illustrate our interpretation of forest dynamics. The NDVI profile is accompanied by the Landsat imagery stack in false-color infrared (near-infrared, short-wave infrared, and red assigned to the RGB channels), showing one image subset per year (1985 – 1987, 1992, and 1998 – 2020). The black circles indicate the analyzed pixel and its surrounding neighborhood (10 x 10 cell window). The black arrow shows the start of the dense time series, and the chips with a red outline correspond to the red points in the time series, indicating a year with a possible disturbance. In addition, a clip of the UAV orthomosaic showing the area of the study plot (314 m^2) as a red circle. Below this information, there is text structured in three paragraphs, commenting on the NDVI profile, Landsat Imagery, and field notes.

The color palette of the Landsat imagery is described through a comparison between the pixels that cover the plot and the rest of the pixels. Therefore, when we refer to brightness and saturation, it is in relation to the other pixels of the same chip, whose vegetation cover type is interpreted with the available data. Nevertheless, general trends were considered in only a few cases.

Example of group n° 1 (mature, moderately dense, with second age class) – A3 study plot. The highlighted values in 2012, 2018, and 2019 were disregarded and marked as not meaningful, but 1999's value was confirmed as a meaningful outlier showing a strong decrease in NDVI. Subsequently, the signal shows fluctuations, probably due to the effect of the understory (figure 4). In 1999, plot colors turned greenish and desaturated compared to the previous date. In this band combination, healthy vegetation appears reddish (particularly, lenga crown cover appears orange-red). This confirms that the 1999 outlier is a trustworthy data point.

The field data collected in 2020 describe the 10 m radius study plot as a light forest stand, with few mature trees standing, no abundant second age class, and nearby regeneration patches. The study plot is located in a sector that has been formerly managed with tending cuts, so the cover reduction is attributed to human intervention.

*Example of group no. 2 (mature, moderately dense, without second age class) – B2 study plot***.** The NDVI profile showed high variability, starting slightly above 0.8, which is a value that full stocked plots have shown, such as B3 and I1 (figure 5). Subsequently, it drops in 1999 to a value close to 0.7. Subsequently, it fluctuates below 0.8. We attribute the increase after 2014 to a radiometric difference caused by the inclusion of L8 in the time series (this effect can be clearly observed in D2 and C4, among others). The plot is very close to where a path apt for four-wheel-drive vehicles is currently located, and a clear pattern suggesting the opening of that path around 1987 can be seen in the chips (this can also be observed in B3).

Field data indicated that the reduced canopy cover was mainly due to human intervention, as felled stems were seen in the plot, as well as human-induced standing dead trees. This is a common practice in lenga forests, where old and deteriorated trees are ring-barked to favor the growth of natural regeneration below. Observed regeneration is very scarce.

Example of group no. 3 (mature, dense, with second age class) – B3 study plot. This plot shows the most stable conditions throughout the time series analysis (mean = 0.855 and SD = 0.0267, Figure 6). Therefore, B3 was used to

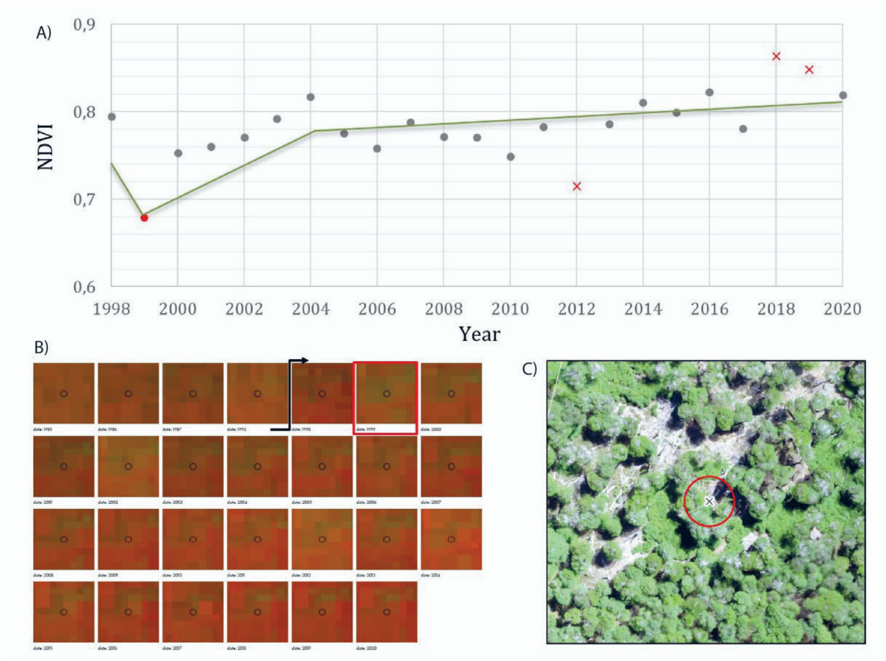

Figure 4. Plot A3 (for plot labels, see figure 2). A) Spectral time series trajectory plot; B) Landsat imagery stack; C) A true-colour orthomosaic (circle radius is 10 m). Gap dynamics due to former tending cuts leading to a light forest stand, with few mature trees standing, no abundant second age class, and nearby regeneration patches in 2020.

Parcela A3. A) Trayectoria temporal de la respuesta espectral de la parcela; B) Serie de imágenes Landsat; C) Ortomosaico de color real (el círculo tiene un radio de 10 m). Dinámica de claros ocasionada por un primer raleo que está conduciendo a un rodal con menos stock y pocos árboles maduros, sin una clase secundaria abundante, y, en 2020, se detectan parches de regeneración cercanos a la parcela.

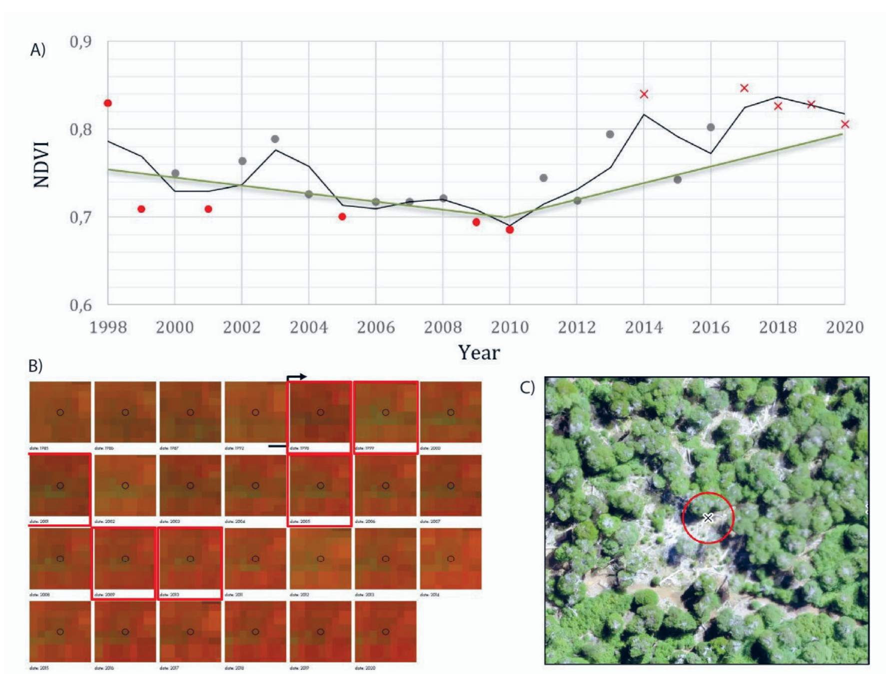

Figure 5. Plot B2. A) Spectral time series trajectory plot; B) Landsat imagery stack; C) A true-colour orthomosaic (circle radius is 10 m). Gap dynamics with reduced canopy cover mainly due to human intervention with felled stems as well as human-induced (ring-barked) standing dead trees and scarce regeneration.

Parcela B2. A) Trayectoria temporal de la respuesta espectral de la parcela; B) Serie de imágenes Landsat; C) Ortomosaico de color real (el círculo tiene un radio de 10 m). Dinámica de claros con una reducción de la cobertura del dosel principalmente producida por la intervención humana con volteos y anillado de la corteza de árboles en pie. Regeneración escasa.

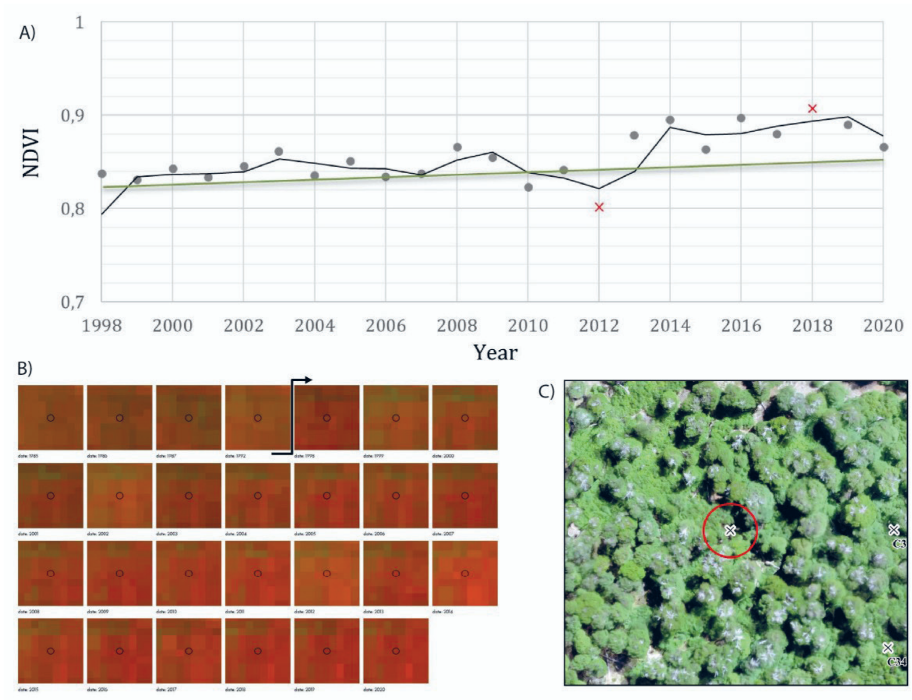

Figure 6. Plot B3. A) Spectral time series trajectory plot; B) Landsat imagery stack; C) A true-colour orthomosaic (circle radius is 10 m). Very stable stand conditions throughout the time series analysis with abundant regeneration as well as mature trees in 2020.

Parcela B3. A) Trayectoria temporal de la respuesta espectral de la parcela; B) Serie de imágenes Landsat; C) Ortomosaico de color real (el círculo tiene un radio de 10 m). Condición muy estable a través de la serie de tiempo con abundante regeneración y árboles maduros en 2020.

identify outliers using the z-score (Equation [2]). The chips include bright unsaturated pixels in the north, where a path suitable for four-wheel-drive vehicles is currently located. Path signals were not observed before 1987. The brightness and saturation of pixels in the plot neighborhood change, but the plot itself is bright and saturated on all chips. The data collected in 2020 during the field visit show that the study plot is located at a micro-relief zone, near a small stream, showing abundant regeneration as well as mature trees.

Example of group no. 4 (mature, dense, with scarce second age class) – D2 study plot. In 1999, the NDVI showed a strong reduction, which was consistently observed in 2000 and 2001 (figure 7). Until 2006, the NDVI was clearly below 0.8. Subsequently, there was a slow increase to reach a plateau. We attributed the increase after 2014 to a radiometric difference caused by the inclusion of L8 in the time series. The colors do not show any clear or meaningful patterns. From the collected field data, the reduction in canopy cover may have been due to wind or snow damage, as there was evidence of natural breakage of the trees. However, according to scarce management records, human interventions are not discarded.

Example of group no. 5 (mature, dense, without second age class) – I1 study plot. All highlighted NDVI values were disregarded due to technical errors (cloud or satellite distortion of values). The remaining data points showed a constant NDVI slightly above 0.8 (in figure 8). The plot was covered with saturated light red color throughout the series. There were no visible severe changes, even in the years before the dense time series (before 1998). These observations strongly suggest a uniform cover of tree crowns across the years. Field notes describe the study plot as a mature forest stand with a canopy cover of approximately 0.7, no regeneration, no coarse woody debris, and no disturbance evidence.

Example of group no. 6 (young, dense, without second age class) – C4 study plot. The trajectory dynamics show slow and consistent growth following a non-severe canopy reduction in 1999 and the early 2000s (figure 9). Overall, the saturation and brightness of the chips increased over the years, which matched the NDVI profile trends. The clearest pattern was an increase in the texture of the chips in the form of a greater range of brightness. This suggests that more east shadows affecting the signal, which is an indication of crown development.

From the field notes, there is speculation about the presence of two age groups of regeneration, which may indicate a second disturbance phase before 1998. The limited management records available suggest that disturbances were caused by human intervention. Overall, it appears that a seedling bank was present prior to the disturbance.

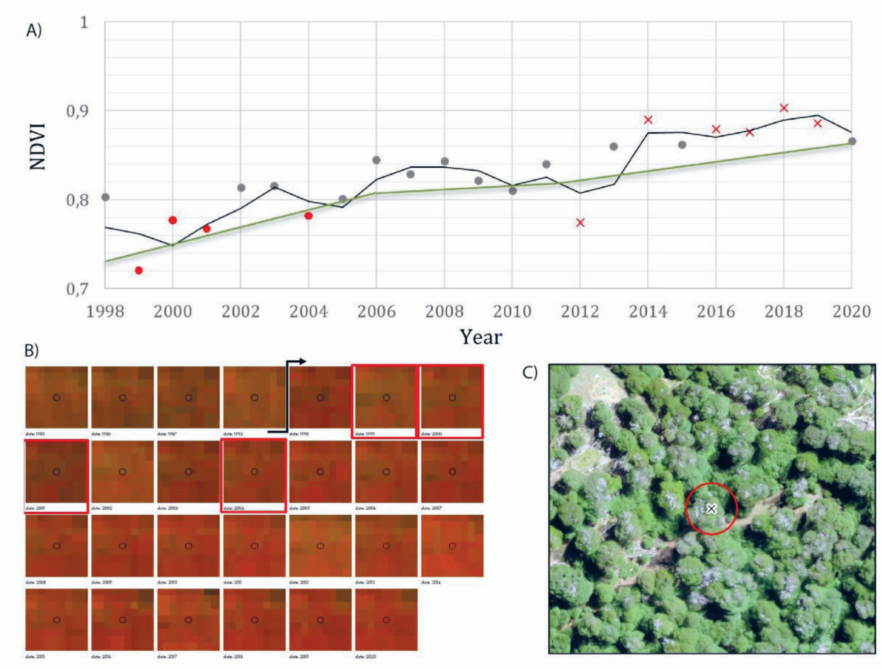

Figure 7. Plot D2. A) Spectral time series trajectory plot; B) Landsat imagery stack; C) A true-colour orthomosaic (circle radius is 10 m). Gap dynamics reflected by the reduction of the canopy cover, probably due to wind or snow damage (evidence of natural breakage of the trees); human intervention, however, is not discarded.

Parcela D2. A) Trayectoria temporal de la respuesta espectral de la parcela; B) Serie de imágenes Landsat; C) Ortomosaico de color real (el círculo tiene un radio de 10 m). Dinámica de claros reflejada por la reducción de la cobertura del dosel, probablemente debido a daños por viento o nieve (evidencia de desmoronamiento de copas); sin embargo, no se descarta la intervención humana.

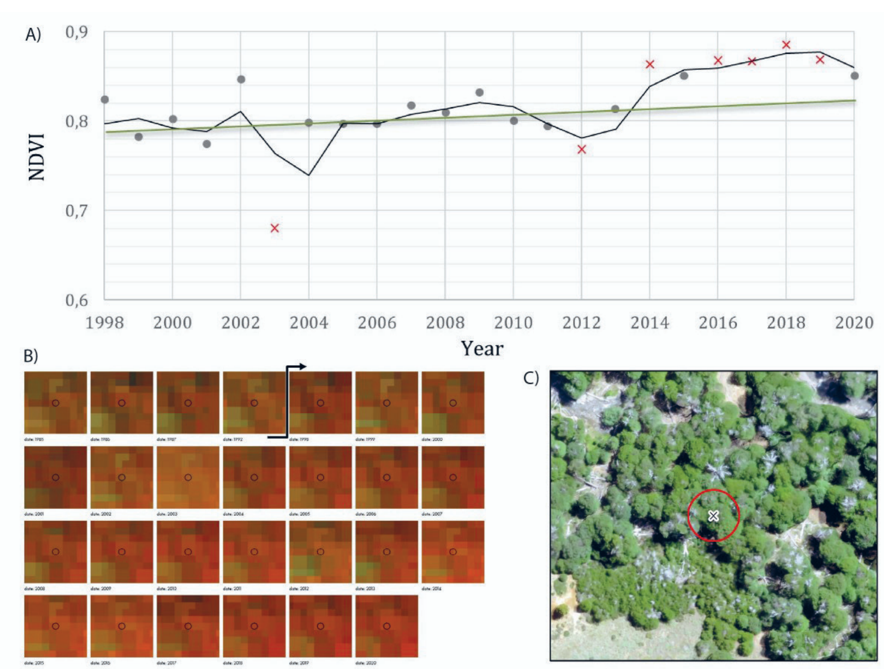

Figure 8. Plot I1. A) Spectral time series trajectory plot; B) Landsat imagery stack; C) A true-colour orthomosaic (circle radius is 10 m). Uniform cover of tree crowns across the years with a mature forest stand, no regeneration, no coarse woody debris, and no disturbance evidence in 2020.

Parcela I1. A) Trayectoria temporal de la respuesta espectral de la parcela; B) Serie de imágenes Landsat; C) Ortomosaico de color real (el círculo tiene un radio de 10 m). Cobertura uniforme de copas a lo largo de los años con un rodal maduro, sin regeneración, sin madera muerta gruesa, y sin evidencia de disturbios en 2020.

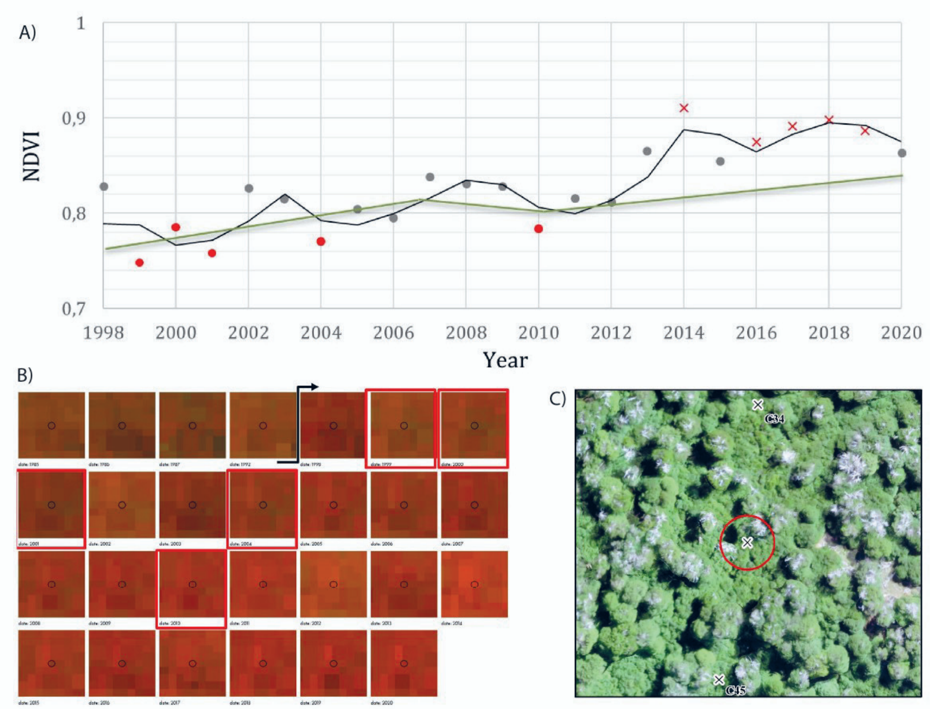

Figure 9. Plot C4. A) Spectral time series trajectory plot; B) Landsat imagery stack; C) A true-colour orthomosaic (circle radius is 10 m). Slow and consistent growth following a non-severe canopy reduction in 1999 and early 2000s and the presence of two age groups of regeneration in 2020, probably by former human intervention.

Parcela C4. A) Trayectoria temporal de la respuesta espectral de la parcela; B) Serie de imágenes Landsat; C) Ortomosaico de color real (el círculo tiene un radio de 10 m). Lento y consistente crecimiento seguido de una reducción no severa del dosel en 1999 y comienzos de los años 2000 y la presencia de dos estratos de regeneración en 2020, probablemente debido a intervenciones humanas previas.

DISCUSSION

Forest dynamics can result from any combination of short-term events (*i.e.* windthrows and seasonal droughts) and long-term effects related to climate change and continuous human activities (*i.e.* forest grazing and branch dieback) (Banskota *et al.* 2014). Remote sensing provides a tool for observing and monitoring signals that are linked to those effects and, by doing so, provides methods to identify the time and intensity of disturbances. However, this should not be pursued without considering the uncertainties inherent in linking the signal to the required information. Another aspect to consider is the relatively shallow depth of the image archive, considering the age of the forests. Nevertheless, no other methodology has an archive as complete as this for virtually any forested location.

In our study, we used time series as a tool for identifying disturbances in a given period by, integrating the BAP algorithm and the TimeSync method. We used this methodology to detect the dynamics of small-scale lenga forests. Starting by eliminating gross errors, due to satellite failures or algorithm flaws, we followed a step-down (scale-wise) process to evaluate the time series. By examining a spectral time-series trajectory plot and Landsat imagery, supported by field data, a UAV orthomosaic, and expert knowledge, we were able to interpret the gap dynamics in the Huemules Experimental Unit. In our study, the proposed z-score approach to identifying outliers based on a previously identified stable plot was the key to achieving our goal.

During the plot-to-plot examination, variability in vegetation structure could be observed. There were patches with no regeneration, patches with high regeneration, and mixtures. The variability was sufficient to create a patchy vegetation structure, typical of the natural lenga dynamics observed in central and north Patagonia. This has also been reported in European primaeval beech forests (Korpel 1995). Studies on the regeneration of lenga forests point to the necessity of gaps (Rosenfeld *et al.* 2006). As practice also in European beech and mixed oak-beech forests (Bílek *et al.* 2014), silvicultural practices for the regeneration of forest stands can and should adapt to its natural gap dynamics.

The mature stands with the presence of a second tree layer had stable time series dynamics, either having no canopy structure change in the whole time series or following a low crown reduction in 1999 or the early 2000s. Our approach proved to be useful for identifying the time and intensity of crown cover reduction and the dynamics of forest stands. However, the identification of gap dynamics through analysis and interpretation of satellite images has limitations. Satellite images do not allow us to identify the type of crown-cover reduction. Therefore, field checks are necessary.

In the case of gradual forest change (*i.e.* as a consequence of climate change), our methodology may prove useful solely by observing value fluctuations if a solid baseline is built and satellite differences are calibrated. As indicated by Vogelmann *et al.* (2016), the interpretation of the Landsat time series provides an opportunity to quantify and understand more gradual forms of forest disturbance, such as insect, disease, and drought, induced mortality. Consequently, annual forest canopy decline data developed by Landsat time-series interpretation offers an opportunity to assess the contribution of climatic variation to forest change, which is not generally possible using traditional field-based forest inventory data (Bell *et al.* 2018).

Any improvement in satellite radiometry has the potential to introduce bias in the time series, which can be misinterpreted as a signal with biological meaning. For instance, we observed an overall NDVI increase after 2014, matching the incorporation of Landsat 8 data into the time series. This bias breaks the continuity of the time-series. However, theoretically, this could be avoided by examining the time series in two sections before and after the new satellite. In addition, the Scan Line Corrector (SLC) failure induced challenges in building coherent dense time series.

In this study, we focused on the application and adaptation of the TimeSync method to detect and interpret fine-scale forest gap dynamics. The critical evaluation of LandTrendr applied to this domain and the eventual development of an improved approach to LandTrendr will be a challenging objective for future research. In addition, further research could be oriented toward using Sentinel data to complement the Landsat archive. However, substantial research is needed to ensure a seamless transition between Sentinel data and the Landsat archive. To date, Landsat 8 OLI offers outstanding continuity to the mission and, aside from the greater resolution of Sentinel data, it is unclear how advantageous it would be to include Sentinel data. A new generation of remote sensing data, such as the Global Ecosystem Dynamics Investigation's (GEDI) Light Detection and Ranging (LiDAR) system and SAOCOM (Satélite Argentino de Observación Con Microondas = Argentine Microwaves Observation Satellite) (*i.e.* Seppi *et al.* 2022), could be incorporated as an additional data source to be interpreted in the same manner as the drone imagery was added in our study, that is, relying on human expert knowledge and the extraordinary ability of the human brain to interpret images.

CONCLUSIONS

There is increasing consensus about the need to embrace forest management practices that mimic forest natural gap dynamics to preserve ecosystem services. The methods analyzed here can contribute to enhancing the field characterizations of natural gap dynamics and, therefore, contribute to sustainable forest management. The method proved to be a useful, cost-effective, and rapid tool for identifying the time and intensity of satellite signal variations in the Landsat archive. However, uncertainty remains in the biological meaning of satellite signals. Therefore, identifying the drivers of these trends solely by remote analysis is an unsolved methodological challenge.

ACKNOWLEDGMENTS

We thank Martin Rutzinger (University of Innsbruck) for his support and Rodrigo Principe for providing assistance with the use of his package, *geebap*.

AUTHOR CONTRIBUTIONS

GD, SZ: Conceptualization; VK, GD, DM: Data curation; VK, GD, DM: Investigation & Methodology; GD, DM: Software; VK, SZ: Original draft; VK, GD, DM, SZ: Review and editing.

FUNDING

This study was financially supported by the University of Innsbruck through a "*Kurzfristige Wissenschaftliche Arbeiten im Ausland* (KWA)" scholarship.

REFERENCES

Amoroso MM, AP Blazina. 2020. Disturbance history and dynamics of an old-growth *Nothofagus* forest in Southern Patagonia. *Forests* 11: 101. DOI: https://doi.org/10.3390/f11010101

Armesto J, I Casassa, O Dollenz. 1992. Age structure and dynamics of Patagonian beech forests in Torres Del Paine National Park, Chile. *Vegetatio* 98: 13-22. DOI: https://doi.org/10.1007/BF00031633

Baker DJ, G Richards, A Grainger, P Gonzalez, S Brown, R DeFries, A Held, J Kellndorfer, P Ndunda, D Ojima, PE Skrovseth, C Souza, F Stolle. 2010. Achieving forest carbon information with higher certainty: A five-part plan. *Environmental Science & Policy* 13: 249-260. DOI: https://doi.org/10.1016/j.envsci.2010.03.004

Banskota A, N Kayastha, MJ Falkowski, MA Wulder, RE Froese, JC White. 2014. Forest monitoring using Landsat Time Series data: A review. *Canadian Journal of Remote Sensing* 40: 362-384. DOI: https://doi.org/10.1080/07038992.2014.987376

Bell DM, WB Cohen, M Reilly, Z Yang. 2018. Visual interpretation and time series modeling of Landsat Imagery highlight drought's role in forest canopy declines. *Ecosphere* 9: e02195. DOI: https://doi.org/10.1002/ecs2.2195

Bílek L, J Remeš, V Podrázský, D Rozenbergar, J Diaci, D Zahradník. 2014. Gap regeneration in near-natural European beech forest stands in Central Bohemia – the role of heterogeneity and micro-habitat factors. *Dendrobiology* 71: 59-71. DOI: https://doi.org/10.12657/denbio.071.006

Brockerhoff EG, L Barbaro, B Castagneyrol, DI Forrester, B Gardiner, JR González-Olabarria, P Lyver, N Meurisse, A Oxbrough, H Taki, ID Thompson, F van der Plas, H Jactel. 2017. *Forest* biodiversity, ecosystem functioning and the provision of ecosystem services. *Biodiversity and Conservation* 26: 3005-3035. DOI: https://doi.org/10.1007/s10531-017-1453-2

CIEFAP and MAyDS. 2016. Actualización de la clasificación de tipos forestales y cobertura del suelo de la región Bosque Andino Patagónico. Informe final. Update of the classification of forest types and land cover of the Andean Patagonian Forest region. Final Report. CIEFAP, Esquel, 111 p. Accessed on 5 May 2018. Available in https://www.argentina.gob.ar/sites/default/files/informe_final_ccs_bap_20160712.pdf

Cohen WB, Z Yang, R Kennedy. 2010. Detecting trends in forest disturbance and recovery using yearly Landsat Time Series: 2. TimeSync - Tools for calibration and validation. *Remote Sensing of Environment* 114: 2911-2924. DOI: https://doi.org/10.1016/j.rse.2010.07.010

Díaz GM, D Mohr-Bell, M Garrett, L Muñoz , JD Lencinas. 2020. Customizing Unmanned Aircraft Systems to reduce forest inventory costs: Can oblique images substantially improve the 3D reconstruction of the canopy? *International Journal of Remote Sensing* 41: 3480-3510. DOI: https://doi.org/10.1080/01431161.2019.1706200

Foga S, PL Scaramuzza, S Guo, Z Zhu, RD Dilley, T Beckmann, GL Schmidt, JL Dwyer, MJ Hughes, B Laue. 2017. Cloud detection algorithm comparison and validation for operational Landsat data products. *Remote Sensing Environment* 194: 379-390. DOI: https://doi.org/10.1016/j.rse.2017.03.026

Ghazoul J, R Chazdon. 2017. Degradation and recovery in changing forest landscapes: A Multiscale Conceptual Framework. *Annual Review of Environment and Resources* 42(1): 161-188. DOI: https://doi.org/10.1146/annurev-environ-102016-060736

Griffiths P, S van der Linden, T Kuemmerle, P Hostert. 2013. A pixel-based Landsat compositing algorithm for large area land cover mapping. *IEEE Journal of Selected Topics in Applied Earth Observations and Remote Sensing* 6: 2088-2101. DOI: https://doi.org/10.1109/JSTARS.2012.2228167

Hirschmugl M, H Gallaun, M Dees, P Datta, J Deutscher, N Koutsias, M Schardt. 2017. Methods for mapping forest disturbance and degradation from optical earth observation data: A review. *Current Forestry Reports* 3: 32-45. DOI: https://doi.org/10.1007/s40725-017-0047-2

Huang C, SN Goward, JG Masek, N Thomas, Z Zhu, JE Vogelmann. 2010. An automated approach for reconstructing recent forest disturbance history using dense Landsat time series stacks. *Remote Sensing of Environment* 114: 183-198. DOI: https://doi.org/10.1016/j.rse.2009.08.017

Kennedy RE, WB Cohen, TA Schroeder. 2007. Trajectory-based change detection for automated characterization of forest disturbance dynamics. *Remote Sensing of Environment* 110: 370-386. DOI: https://doi.org/10.1016/j.rse.2007.03.010

Kennedy RE, Z Yang, WB Cohen. 2010. Detecting trends in forest disturbance and recovery using yearly Landsat time series: 1. LandTrendr - temporal segmentation algorithms. *Remote Sensing of Environment* 114: 2897-2910. DOI: https://doi.org/10.1016/j.rse.2010.07.008

Korpel S. 1995. Die Urwälder der Westkarpaten. Stuttgart, Jena, New York. Fischer. 310 p.

McCarthy J. 2001. Gap dynamics of forest trees: A review with particular attention to boreal forests. *Environmental Reviews* 9: 1-59. DOI: https://doi.org/10.1139/er-9-1-1

Mundo IA, R Villalba, TT Veblen, T Kitzberger, A Holz, J Paritsis, A Ripalta. 2017. Fire history in southern Patagonia: human and climate influences on fire activity in *Nothofagus pumilio* forests. *Ecosphere* 8(9): e01932. DOI: https://doi.org/10.1002/ecs2.1932

Novo-Fernández A, S Franks, C Wehenkel, PM López-Serrano, M Molinier, CA López-Sánchez. 2018. Landsat time series analysis for temperate forest cover change detection in the Sierra Madre Occidental, Durango, Mexico. *International Journal of Applied Earth Observation and Geoinformation* 73: 230-244. DOI: https://doi.org/10.1016/j.jag.2018.06.015

Pacha MJ, S Luque, L Galetto, L Iverson. 2007. Understanding biodiversity loss: An overview of forest fragmentation in South America. *IALE Landscape Research and Management papers. International Association of Landscape Ecology*. ISSN: 1570-6532

Principe R. 2017. Best Available Pixel Composite using the Python API of Google Earth Engine (GEE). CIEFAP-MAyDS, Esquel. Accessed on 15 March 2019. Available in https://github.com/fitoprincipe/geebap

Project Jupyter. 2021. The Jupyter Notebook. Jupyter, Paris. Accessed on 24 June 2022. Available on https://jupyter.org/

Pugh TAM, R Seidl, D Liu, M Lindeskog, LP Chini, C Senf. 2024. The anthropogenic imprint on temperate and boreal forest demography and carbon turnover. *Global Ecology and Biogeography* 33: 100-115. DOI: https://doi.org/10.1111/geb.13773

Python Software Foundation. 2021. The Python Tutorial. Python Software Foundation, Wilmington, USA. Accessed on 2 October 2022. Available in https://docs.python.org/

Quinteros CP. 2018. Propiedades ecosistémicas de bosques de *Nothofagus pumilio* afectadas por diferente intensidad de uso ganadero en Chubut, Patagonia Argentina (Ecosystem properties of *Nothofagus pumilio* forests affected by different intensities of livestock in Chubut, Patagonia, Argentina). *Ecosistemas* 27: 24-32. DOI: https://doi.org/10.7818/ECOS.1483

Ramírez C, I Alberdi, C Bahamondez, J Freitas. 2022. National forest inventories of Latin America and the Caribbean – Towards the harmonization of forest information. Rome, FAO. Available in https://doi.org/10.4060/cb7791en

Rosenfeld JM, RM Navarro Cerrillo, JR Guzman Alvarez. 2006. Regeneration of *Nothofagus pumilio* [Poepp. *et* Endl.] Krasser forests after five years of seed tree cutting. *Journal of Environmental Management* 78: 44-51. DOI: https://doi.org/10.1016/j.jenvman.2005.03.009

Salgado Salomón ME, C. Barroetaveña, M. Rajchenberg. 2013. *Pseudotsuga menziesii* invasion in native forests of Patagonia, Argentina: What about mycorrhizas? *Acta Oecologica* 49: 5-11. DOI: https://doi.org/10.1016/j.actao.2013.01.018

Seppi SA, C López-Martinez, MJ Joseau. 2022. Assessment of L-band SAOCOM InSAR coherence and its comparison with C-band: A case study over managed forests in Argentina. *Remote Sensing* 14: 5652. DOI: https://doi.org/10.3390/rs14225652

Sturtevant BR, M-J Fortin. 2021. Understanding and modeling forest disturbance interactions at the landscape level. *Frontiers in Ecology and Evolution* 9: 653647. DOI: https://doi.org/10.3389/fevo.2021.653647

Townshend JRG, CO Justice. 1988. Selecting the spatial resolution of satellite sensors required for global monitoring of land transformations. *International Journal of Remote Sensing* 9: 187-236. DOI: https://doi.org/10.1080/01431168808954847

Vogelmann JE, AL Gallant, H Shi, Z Zhu. 2016. Perspectives on monitoring gradual change across the continuity of Landsat sensors using time-series data. *Remote Sensing of Environment* 185: 258-270. DOI: https://doi.org/10.1016/j.rse.2016.02.060

White JC, MA Wulder, GW Hobart, JE Luther, T Hermosilla, P Griffiths, NC Coops, RJ Hall, P Hostert, A Dyk, L Guindon. 2014. Pixel-based image compositing for large-area dense time series applications and science. *Canadian Journal of Remote Sensing* 40: 192-212. DOI: https://doi.org/10.1080/07038992.2014.945827

Wulder MA, JG Masek, WB Cohen, TR Loveland, CE Woodcock. 2012. Opening the archive: How free data has enabled the science and monitoring promise of Landsat. *Remote Sensing Environment* 122: 2-10. DOI: https://doi.org/10.1016/j.rse.2012.01.010

Zeberio JM, CA Pérez. 2020 Rehabilitation of degraded areas in northeastern Patagonia, Argentina: Effects of environmental conditions and plant functional traits on performance of native woody species. *Journal of Arid Land* 12, 653–665. DOI: https://doi.org/10.1007/s40333-020-0021-x

Zerbe S, ST Storz, G. Leitinger, NZ Joelson, J Bava, S Heinrichs, C Leuschner, G Loguercio, A Simon, MF Urretavizcaya, H Walentowski. 2023. Regeneration of *Nothofagus dombeyi* (Mirb.) Ørst. in little to moderately disturbed southern beech forests in the Andes of Patagonia (Argentina). *Forest Ecosystems* 10: 100126. DOI: https://doi.org/10.1016/j.fecs.2023.100126

Recibido: 02/10/2023
Aceptado: 27/07/2024